AMSR-E/AMSR2 Unified L3 Daily 25 km Brightness Temperatures & Sea Ice Concentration Polar Grids, Version 1

USER GUIDE

How to Cite These Data

As a condition of using these data, you must include a citation:

Markus, T., J. C. Comiso, and W. N. Meier. 2018. *AMSR-E/AMSR2 Unified L3 Daily 25 km Brightness Temperatures & Sea Ice Concentration Polar Grids, Version 1*. [Indicate subset used]. Boulder, Colorado USA. NASA National Snow and Ice Data Center Distributed Active Archive Center. https://doi.org/10.5067/TRUIAL3WPAUP. [Date Accessed].

FOR QUESTIONS ABOUT THESE DATA, CONTACT NSIDC@NSIDC.ORG

FOR CURRENT INFORMATION, VISIT https://nsidc.org/data/AU_SI25

National Snow and Ice Data Center

TABLE OF CONTENTS

1 DATA DESCRIPTION

1.1 Parameters

This data set consists of the following gridded parameters:

- Vertical and horizontal brightness temperatures (referred to as Tb or TB in this document) for the following channels, with separate HDF-EOS5 fields for afternoon ascending orbits, morning descending orbits, and full orbit daily averages:
  - 6.9 GHz
  - 10.7 GHz
  - 18.7 GHz
  - 23.8 GHz
  - 36.5 GHz
  - 89.0 GHz
- Arctic sea ice concentration using the NASA Team 2 (NT2) algorithm, with separate fields for ascending orbits, descending orbits, and daily averages.
- Antarctic sea ice concentration using the NT2 algorithm, with separate fields for ascending orbits, descending orbits, and daily averages.
- Arctic sea ice concentration differences between the Bootstrap Algorithm and the NT2 algorithm, with separate fields for ascending orbits, descending orbits, and daily averages.
- Antarctic sea ice concentration differences between the Bootstrap Algorithm and the NT2 algorithm, with separate fields for ascending orbits, descending orbits, and daily averages.

1.1.1 Parameter Details

Brightness temperature data have a scale factor of 0.1. Multiply data values by 0.1 to obtain T_b in kelvin (K).

Brightness temperature values:

- 0: Missing or out-of-bounds data
- 50-320 K: Valid T_bs in Kelvin (K).

Sea ice concentration values:

- 0: Open Water
- 1 - 100: Percent sea ice concentration
- 110: Missing data
- 120: Land

Sea ice difference values between the Bootstrap and NT2 Algorithms:

- 0: Bootstrap sea ice concentration is equal to the NT2 concentration
- 1 - 100: Bootstrap sea ice concentration is greater than NT2 concentration
- -1 to -100: Bootstrap sea ice concentration is less than NT2 concentration
- 110: Missing data
- 120: Land

1.2 File Information

1.2.1 Format

Data are in HDF-EOS5 32-bit signed integer format. For software and more information, visit the HDF-EOS website.

1.2.2 File Contents

Sample data images.

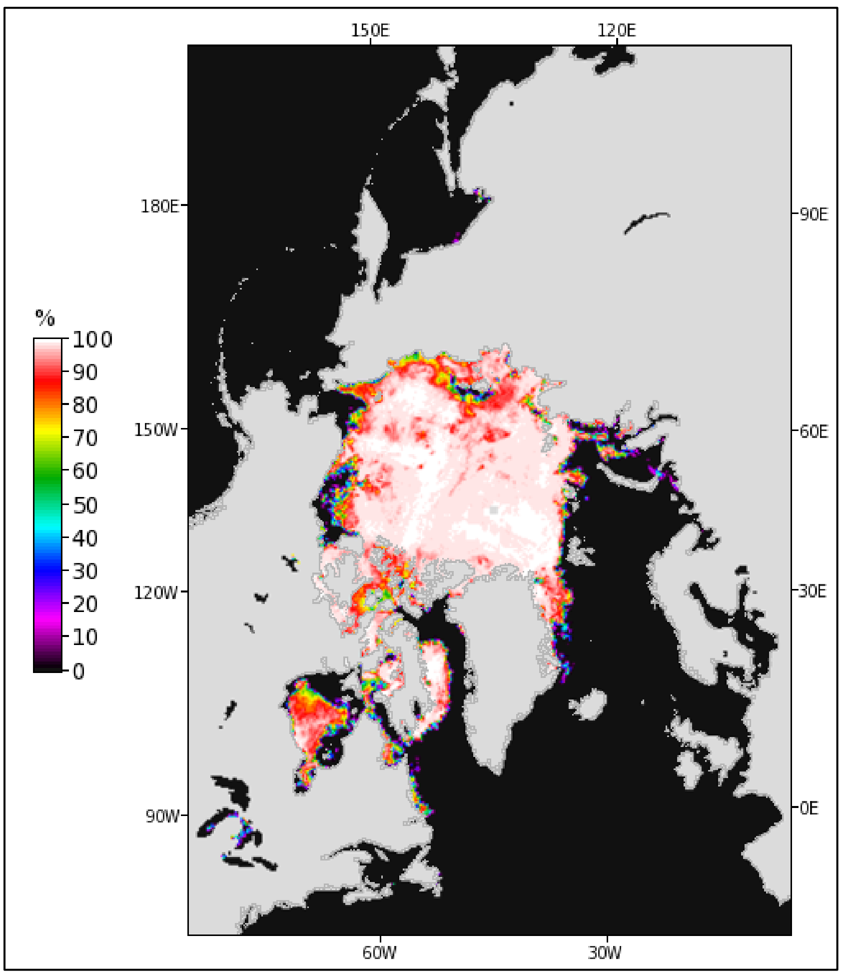

Figure 1. Land, Atmosphere Near-real-time Capability for EOS (LANCE) image of AMSR2 Northern Hemisphere 25 km Sea Ice Concentration for 23 June 2016. File name: AMSR_2_L3_SeaIce25km_R00_20160623_N_CON.png

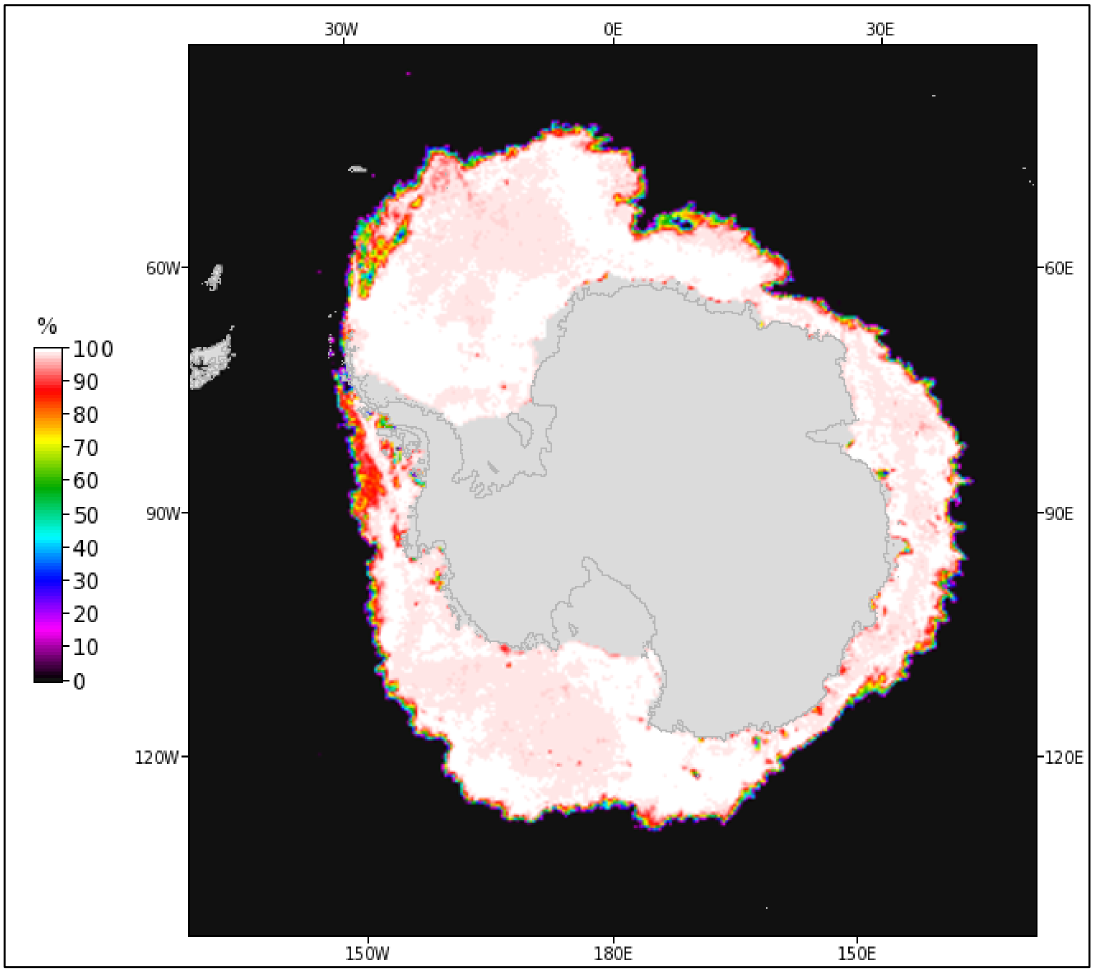

Figure 2. LANCE image shows AMSR2 Southern Hemisphere 25 km Sea Ice Concentration for 23 June 2016.
File name: AMSR_2_L3_SeaIce25km_R00_20160623_S_CON.png

1.2.3 Directory Structure

Each data file includes 84 parameter fields (42 Northern Hemisphere and 42 Southern Hemisphere), and three metadata fields (CoreMetadata, StructMetadata, and Processing_Facility). The figure below shows a subset of these parameter fields.

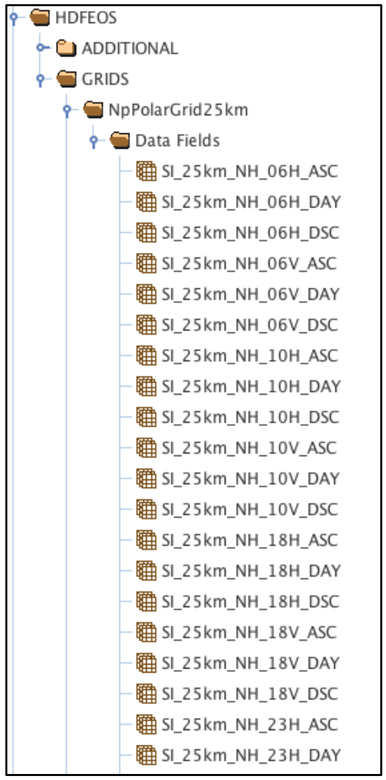

Figure 3. a subset of the Northern Hemisphere parameter fields.

1.2.4 Ancillary Data

There are two ancillary text files (.qa and .ph) included with each day of data. The .qa text file provides a quality assessment summary. The .ph text file provides a list of the input data files.

1.2.5 Naming Convention

The parameter name variable values use the parameter convention example below.

Example 1 parameter convention: `SI_25km_HE_PARAM_TIME`

Example 2 parameter name: `SI_25km_NH_89H_ASC`

Table 1. Parameter Name Variables

Variable	Values
`SI`	Indicates sea ice.
`25km`	Indicates a nominal spatial resolution of 25 km.
`HE`	Indicates the observation hemisphere; NH: Northern Hemisphere, SH Southern Hemisphere.

Variable	Values
PARAM	Indicates the measured parameter; 6 GHz, 10 GHz, 18 GHz T_bs, 23 GHz T_bs, 36 GHz T_bs, 89 GHz T_bs, ICECON, and ICEDIFF. Brightness Temperature parameters also include a polarization identifier; V: Vertical and H: Horizontal.
TIME	Indicates the observation time period; ASC: 12 hour ascending orbit, DSC: 12-hour descending orbit, DAY: Full orbit daily average

The file name variable values use the file name convention example below.

Example 1 file name: `AMSR_U2_L3_SeaIce25km_B02_20180509.he5`

Table 2. File Name Variables

Variable	Description
AMSR	Advanced Microwave Sounding Radiometer
U	Unified
2	AMSR2
L3	Level-3
25km	Indicates each grid cell has a nominal resolution of 25 km x 25 km
X##	Product Maturity Code and Version (refer to Table 3)
yyyy	Four-digit year
mm	Two-digit month
dd	Two-digit day
he5	Indicates HDF-EOS5 file format

The following table provides the meaning for the product maturity code variable values.

Table 3. Product Maturity Codes

Variables	Description
B	Beta: Indicates a developing algorithm with updates anticipated.
T	Transitional: Indicates the period between Beta and Validated where the product is past the Beta stage, but not ready for validation. At this stage the algorithm matures and stabilizes.
V	Validated: Products are upgraded to Validated once the algorithm is verified and validated by the science team. Validated products have an associated validation stage. Refer to Table 2 in the Naming Conventions section of the AMSR Unified | Version History page for a description of the stages.

1.3 Spatial Information

1.3.1 Coverage

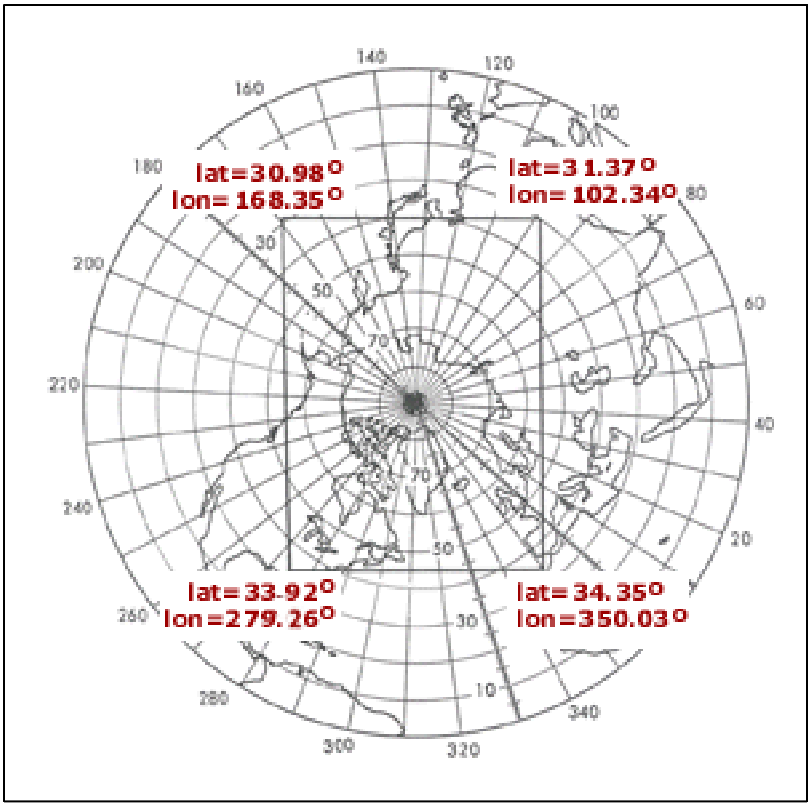

Figure 4. Northern Hemisphere Coverage Extent

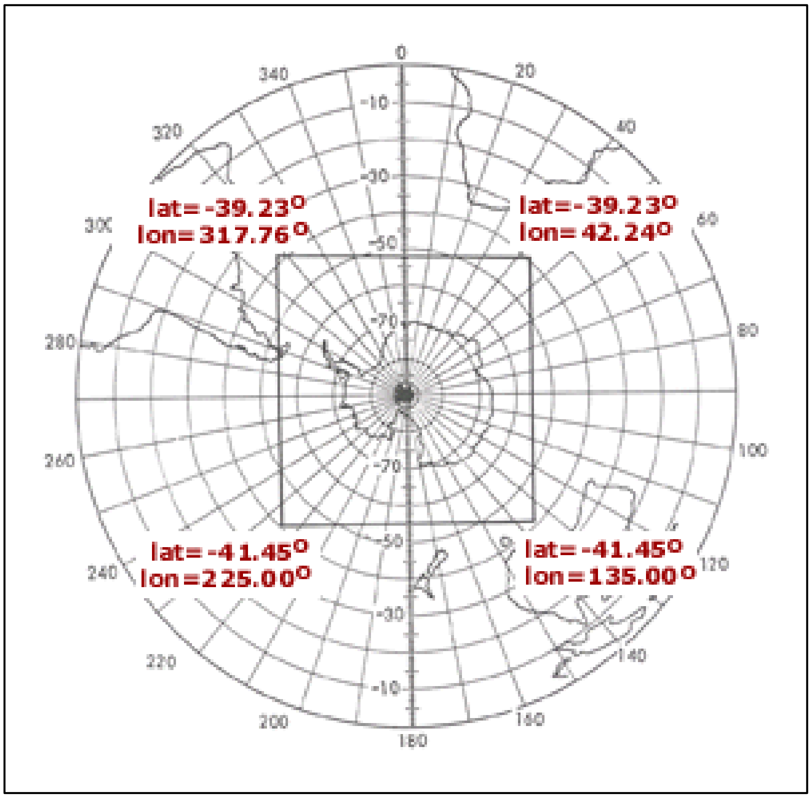

Figure 5. Southern Hemisphere Coverage Extent

Note that a small gap in coverage exists at the poles due to the path of the ascending and descending orbits. Known as the pole hole, this gap is consistent for both AMSR2 and AMSR-E data sets. For additional information see the AMSR-E Pole Hole page.

1.3.2 Resolution

The nominal spatial resolution of the polar grids is 25 km. However, because the polar grids are not equal area, the actual resolution varies by latitude.

1.3.3 Geolocation

The following tables provide information for geolocating this data set.

Table 4. Projection Details

Region	Northern Hemisphere	Southern Hemisphere
Geographic coordinate system	Hughes 1980	Hughes 1980
Projected coordinate system	NSIDC Sea Ice Polar Stereographic North	NSIDC Sea Ice Polar Stereographic South
Longitude of true origin	0	0
Latitude of true origin	70° N	70° S
Scale factor at longitude of true origin	1	1
Datum	Hughes 1980	Hughes 1980
Ellipsoid/spheroid	Hughes 1980	Hughes 1980
Units	Meter	Meter
False easting	0	0
False northing	0	0
EPSG code	3411	3412
PROJ4 string	+proj=stere +lat_0=90 +lat_ts=70 +lon_0=-45 +k=1 +x_0=0 +y_0=0 +a=6378273 +b=6356889.449 +units=m +no_defs	+proj=stere +lat_0=-90 +lat_ts=-70 +lon_0=0 +k=1 +x_0=0 +y_0=0 +a=6378273 +b=6356889.449 +units=m +no_defs
Reference	http://epsg.io/3411	http://epsg.io/3412

Table 5. Grid Details

Region	Northern Hemisphere	Southern Hemisphere
Grid cell size (x, y pixel dimensions)	25 km	25 km
Number of rows	448	332
Number of columns	304	316
Geolocated lower left point in grid	-3850 E, -5350 N	-3950 E, -3950 S
Nominal gridded resolution	25 km	25 km
Grid rotation		
ulxmap – x-axis map coordinate of the center of the upper-left pixel (XLLCORNER for ASCII data)	-3850	-3950
ulymap – y-axis map coordinate of the center of the upper-left pixel (YLLCORNER for ASCII data)	5850	4350

The origin of each x, y grid is the pole. The tables below show the approximate outer boundaries for the Arctic and Antarctic grids. Corner points are listed starting from the upper left corner and progress clockwise. Interim rows define boundary midpoints.

Table 6. Arctic Grid Boundary Details

X (km)	Y (km)	Latitude (deg)	Longitude (deg)	Pixel Location
-3850	5850	30.98	168.35	corner
0	5850	39.43	135.00	midpoint
3750	5850	31.37	102.34	corner
3750	0	56.35	45.00	midpoint
3750	-5350	34.35	350.03	corner
0	-5350	43.28	315.00	midpoint
-3850	-5350	33.92	279.26	corner
-3850	0	55.50	225.00	midpoint

Table 7. Antarctic Grid Boundary Details

X (km)	Y (km)	Latitude (deg)	Longitude (deg)	Pixel Location
-3950	4350	-39.23	317.76	corner
0	4350	-51.32	0.00	midpoint
3950	4350	-39.23	42.24	corner
3950	0	-54.66	90.00	midpoint
3950	-3950	-41.45	135.00	corner
0	-3950	-54.66	180.00	midpoint
-3950	-3950	-41.45	225.00	corner
-3950	0	-54.66	270.00	midpoint

1.3.4 Geolocation Tools

NSIDC provides geolocation tools for polar stereographic data sets. See the Polar Stereo Tools page for more details.

1.3.5 Land Masks

A 25 km Northern Hemisphere land mask called amsr_gsfc_25n.hdf and a 25 km Southern Hemisphere land mask called amsr_nic_25s.hdf are available for use with this product.

1.4 Temporal Information

1.4.1 Coverage

The temporal coverage of this data set extends from 02 July 2012 to the present.

1.4.2 Resolution

Brightness temperatures, sea ice concentrations, and sea ice concentration difference fields are provided in three daily-averaged composites: ascending orbits, descending orbits, and full orbits.

2 DATA ACQUISITION AND PROCESSING

2.1 Background

The AMSR-E/AMSR2 Unified Level-3 T_bs and sea ice concentration products are derived from JAXA AMSR2 Level-1R (L1R) data. These data consist of swath observations from six channels which have been resampled at JAXA. The T_b sensor footprints, also known as the instantaneous field of view (IFOV), vary with frequency. The resampling procedure remaps the T_bs to sets of consistent footprint sizes using the Backus-Gilbert method (Backus et al. 1967). Each resampled set corresponds to the footprint of one frequency and contains that frequency plus all higher-resolution frequencies. Therefore, the number of channels in each resampled set of T_bs varies. See the JAXA Level 1R documentation or Maeda et al. 2016 for more information.

2.2 Processing

2.2.1 Derivation Techniques for Brightness Temperature Grids

2.2.1.1 Source

Brightness temperature grids are derived from the Japan Aerospace Exploration Agency (JAXA) AMSR2 L1R resampled T_b observations from channel: 6.9, 10.7, 18.7, 23.8, 36.5, and 89 GHz. These observations are swath T_bs which are intercalibrated to match the JAXA AMSR-E T_b observations, thus enabling consistent T_bs to be obtained across the JAXA AMSR2 and AMSR-E products.

2.2.1.2 Processing

Swath data from the 6.9, 10.7, 18.7, 23.8, 36.5, and 89 GHz channel are mapped onto the 25 km polar stereographic grid by converting the geodetic latitude and longitude for the center of each scene station, such as the observation footprint, into AMSR2 map grid coordinates. Scene station map grid coordinates determine grid cell assignments. Observations that fall outside the AMSR2 polar grid are ignored. For each grid cell, T_bs observed over a 24-hour period (midnight to midnight Greenwich Mean Time) are summed and then divided by the total number of observations to obtain a daily-averaged T_b value. If no observations fall within a grid cell for a given day, the average T_b is labeled 'missing'. The 24-hour averaging is done three ways: for all ascending orbits, all descending orbits, and a daily average of all orbits.

2.2.2 Derivation Techniques for Sea Ice Concentration Grids

2.2.2.1 Source

Sea ice concentration grids are derived using JAXA AMSR2 L1R resampled T_b observations from channels; 6.9, 10.7, 18.7, 23.8, 36.5 and 89 GHz. These observations are swath T_bs which are adjusted/intercalibrated to match the JAXA AMSR-E T_b observations, thus enabling consistent sea ice parameters to be obtained across the JAXA AMSR2 and AMSR-E products. The use of swath T_bs instead of averaged T_bs is important because atmospheric influence on the T_bs is nonlinear, and the use of averaged T_bs would dilute the atmospheric signal.

Note that the NASA AMSR-E products at the National Snow and Ice Data Center (NSIDC DAAC) currently only use the L2A T_b observations provided by Remote Sensing Systems. In the future, NASA AMSR-E T_b observations and sea ice concentration products may be reprocessed with the unified JAXA L1R T_b observations and archived at NSIDC DAAC.

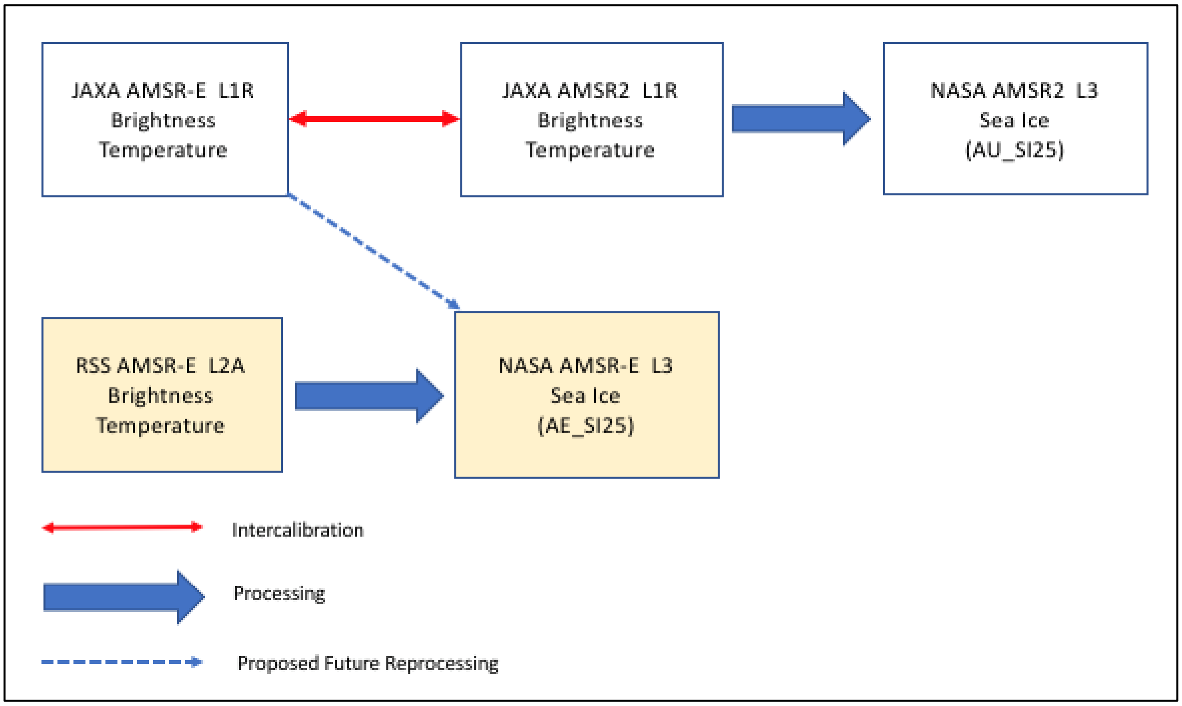

Figure 6. Sources for the NASA AMSR2 L3 (AU_SI25) and NASA AMSR-E L3 (AE_SI25) sea ice concentration products. The NASA AMSR2 L3 sea ice concentration product is derived from JAXA AMSR2 L1R T_bs, which are intercalibrated with JAXA AMSR-E L1R T_bs (boxes with white background). The NASA AMSR-E sea ice concentration product is derived from Remote Sensing Systems AMSR-E L2A T_bs (boxes with yellow background). In the future the NASA AMSR-E L3 sea ice concentration product may be reprocessed using JAXA AMSR-E L1R T_bs.

2.2.2.2 Intercalibration

NASA sea ice estimates derived from AMSR2 T_bs were intercalibrated with NASA sea ice estimates derived from AMSR-E T_bs through a two-step process. First, AMSR-E slow rotation (2 RPM) raw T_bs were used to derive regression equations from co-located pairs of AMSR2 and AMSR-E T_bs. The regression equations are used by the Science Investigator-led Processing Systems (SIPS) to modify AMSR2 T_bs into AMSR-E equivalent T_bs, which are then input into the same NASA Team 2 (NT2) sea ice concentration algorithm that was used for the AMSR-E standard products. The average regression and correlation coefficients used in the AMSR2 processing are provided in Table 1 of the AMSR2 Sea Ice Algorithm Theoretical Basis Document (ATBD), Meier et al. 2017.

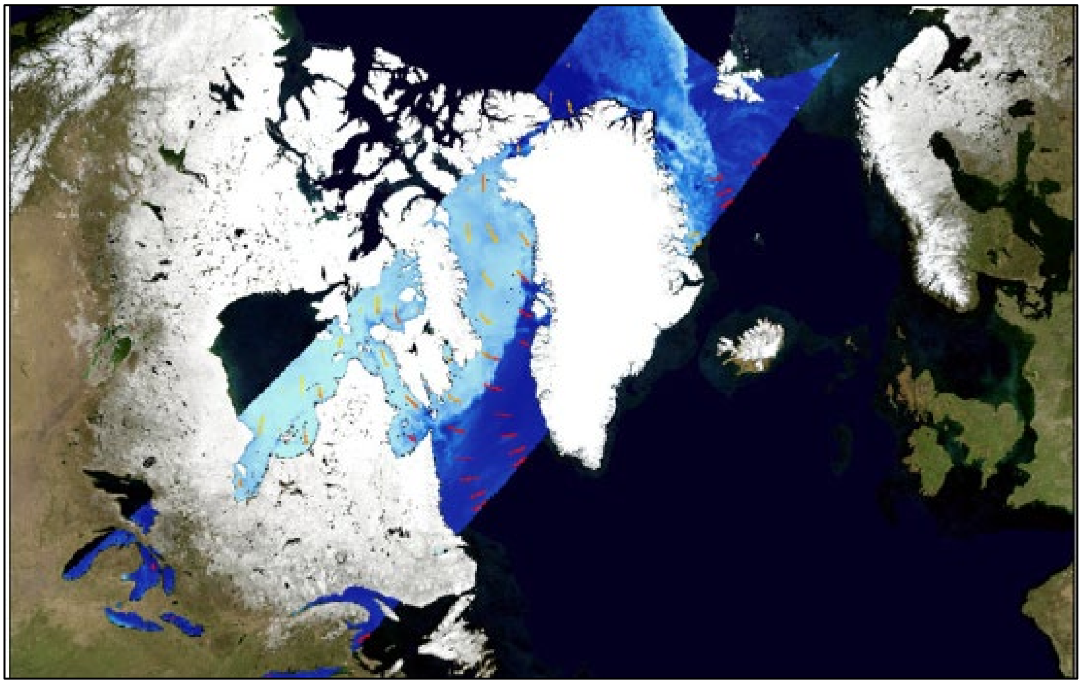

Figure 7. AMSR2 swath from January 2013 overlaid with AMSR-E slow rotation observations shown as red, orange and yellow lines. From January 2013 to January 2014 the AMSR-E instrument continued to operate in slow rotation mode. During this time regression equations were derived from collocated pairs of AMSR2 and AMSR-E T_bs. The regression equations are used to modify AMSR2 T_bs into AMSR-E equivalent T_bs.

2.2.2.3 Algorithm

The sea ice algorithms for AMSR2 are the same as those used for AMSR-E. The only substantial difference is that AMSR2 T_bs are intercalibrated to match AMSR-E T_bs, so that the algorithm coefficients can remain the same and obtain consistent geophysical estimates across both AMSR-E and AMSR2.

The 25 km sea ice concentration product is generated using the Enhanced NASA Team (NT2) algorithm described by Markus et al. 2000 and Markus et al. 2009 for both the Arctic and the Antarctic. The NT2 algorithm uses two ratios of brightness temperatures: polarization ratio (PR) and spectral gradient ratio (GR). These ratios are calculated using the following two equations:

`PR(v) = [TB(vV) – TB(vH)] / [TB(vV) + TB(vH)]` (Equation 3. Polarization Ratio)

`GR(v1pv2p) = TB(v1p) – TB(v2p)] / [TB(v1p) + TB(v2p)` (Equation 4. Spectral Gradient Ratio)

where TB is the brightness temperature at frequency v for the polarized component p: vertical (V) or horizontal (H).

The NT2 algorithm uses these ratios to identify two ice types for the Arctic and Antarctic. In the Arctic, the two ice types correspond to first year ice and multiyear ice. First year ice is defined as ice that has formed since the previous summer. Multiyear ice is defined as ice that has survived at least one summer melt season. In the Antarctic, there is little multiyear ice and the two ice types represent regimes of snow-covered sea ice. The distribution of these ice types is shown in Figure 1 (top section) of the ATBD.

The primary source of error in the original NASA team algorithm was attributed to conditions in the surface layer such as surface glaze and layering (Comiso et al. 1997), which can significantly affect the horizontally polarized 19 GHz T_b (Matzler et al. 1984) leading to increased PR(19) values and thus an underestimate of ice concentration. The use of horizontally polarized channels makes it imperative to resolve a third ice type to overcome the difficulty of these surface effects on the emissivity of the horizontally polarized component of the T_b.

GR(89V19V) and GR(89H19H) are gradient ratios used to resolve the ambiguity between pixels with low ice concentration and pixels with significant surface effects. The difference between these two GRs (ΔGR) is used as a measure of the magnitude of surface effects. Based on this analysis a new ice type is introduced (Type C) which represents ice having significant surface effects (see Figure 1 bottom section in the ATBD).

The NT2 algorithm includes an atmospheric correction scheme as an inherent part of the algorithm. The response of the T_bs to different weather conditions is calculated using an atmospheric radiative transfer model, (Kummerow et al. 1993). Input data for the model are the emissivities of first-year sea ice under winter conditions taken from Eppler et al. 1992, with modifications to achieve agreement between modeled and observed ratios.

Atmospheric profiles are used as another independent variable in the algorithm. There are twelve profiles that include different cloud properties such as cloud base, cloud top, cloud liquid water (Fraser et al. 1975), and average atmospheric temperatures and humidity profiles for summer and winter. The profiles are combined with the radiative transfer model to develop a look-up table of T_b values corresponding to all concentrations (0-100% in 1% intervals) of the two ice types for each of the twelve atmospheric profiles. This results in a model solution space of 101x101x12, or 122,412 possible solutions. For each grid cell, the possible solutions are iterated across to find the solution that best matches the combination of observed T_bs.

2.2.2.4 Weather Filters

Two additional weather filters are applied to correct for severe weather effects over open ocean. These filters are based on spectral gradient ratios, and implemented using threshold values similar to those used by the NT algorithm (Gloersen et al. 1986) and (Cavalieri et al. 1995). Figure 5 in the ATBD shows sea ice concentration maps with and without atmospheric correction.

2.2.2.5 Ocean Climatology Mask

This filter is based on monthly climatological sea surface temperatures (SSTs) from the National Oceanic and Atmospheric Administration (NOAA) ocean atlas. This filter is updated on a monthly basis and removes all ice outside of the SST mask, including land spillover. In the Northern Hemisphere, any pixel where the monthly SST is greater than 278 K is set to zero; whereas in the Southern Hemisphere, any pixel where the monthly SST is greater than 275 K is set to zero.

2.2.2.6 Land Spillover Correction

The spillover of land classified pixels and water classified pixels leads to erroneous ice concentrations along the coast lines adjacent to open water. This makes operational usage of these maps cumbersome. To overcome this difficulty a five-step pixel classification scheme is applied to delineate land pixels from water pixels. See section 3.2.1.2 and Figure 4 in the ATBD for a detailed description of the classification process, and to view ice concentration maps; with and without land spillover correction.

2.2.2.7 Processing

1. Calculate sea ice concentration: To calculate sea ice concentration, the NT2 algorithm is run using the intercalibrated JAXA L1R input T_bs. Brightness temperature values are calculated for each ice concentration and weather combination and, for each of those solutions, the modeled ratios PR (19), PR (89), and ΔGR are calculated. The three observed ratios are then compared with the three modeled ratios. The indices where the differences are smallest will determine the final ice concentration combination.
2. Distinguish new ice from existing ice with surface effects: A gradient ratio (37V19V) with a threshold of –0.02 is used to resolve new ice from existing ice with surface effects (Type C) for pixels where GR(37V19V) is below this threshold, or thin ice for pixels where GR(37V19V) is above this threshold.
3. Apply weather filters: To eliminate severe weather effects over open ocean, weather filters based on the spectral gradient ratio are applied. The threshold for the GR(37V19V) NT weather filter (Gloersen and Cavalieri 1986) is 0.05, where the threshold for the GR(22V19V) NT weather filter (Cavalieri et al. 1995) is 0.045. If the GR values exceed these thresholds, the sea ice concentrations are set to zero.
4. Create sea ice concentration grids: After the algorithm is run on JAXA L1R T_bs, sea ice concentrations are mapped to three polar stereographic grids: one for ascending orbits, one for descending orbits, and one for full orbit daily averages. The gridding of the concentration fields is done using the same drop-in-the-bucket process as the other gridded products.
5. Apply Ocean Climatology Mask: To eliminate low-latitude spurious ice concentrations, Sea Surface Temperatures (SST) filters based on the National Oceanic and Atmospheric Administration (NOAA) monthly ocean atlas are applied.
6. Apply land spillover mask: A land spillover correction scheme is applied to correct for erroneous ice concentrations along coast lines.

For a detailed description of the Algorithm processing for this data set, see section 3.2.1.1 of the ATBD document.

2.2.3 Derivation Techniques for Sea Ice Concentration Difference Grids

Sea ice concentration grids derived from AMSR2 L1R T_bs using the NT2 algorithm (AU_SI25) are compared with sea ice concentration grids derived from AMSR2 L1R T_bs using the Bootstrap algorithm. The sea ice concentration difference is calculated by subtracting the NT2 algorithm from the Bootstrap algorithm (Bootstrap - NT2). The sea ice concentration difference field can be used as an uncertainty measure for the NT2 concentration field; whereas the larger the difference the greater the uncertainty. The difference field also enables users to retrieve the Bootstrap concentration values by adding the concentration difference field to the NT2 concentration field.

The Bootstrap algorithm used here is formulated in the same manner as the Bootstrap Sea Ice Concentration from Nimbus-7 SMMR and DMSP SSM/I-SSMIS Version 3 product. The original Bootstrap algorithm was developed in the 1980s (Comiso, 1986) and the algorithm was later adapted for AMSR-E (Comiso et al, 2003). For a description of the current Version 3 algorithm, see Comiso et al. (2017).

2.2.3.1 Processing

The Bootstrap Algorithm is used in the calculation of sea ice concentration differences between the Bootstrap and the NT2 (Bootstrap-NT2) algorithms for both hemispheres.

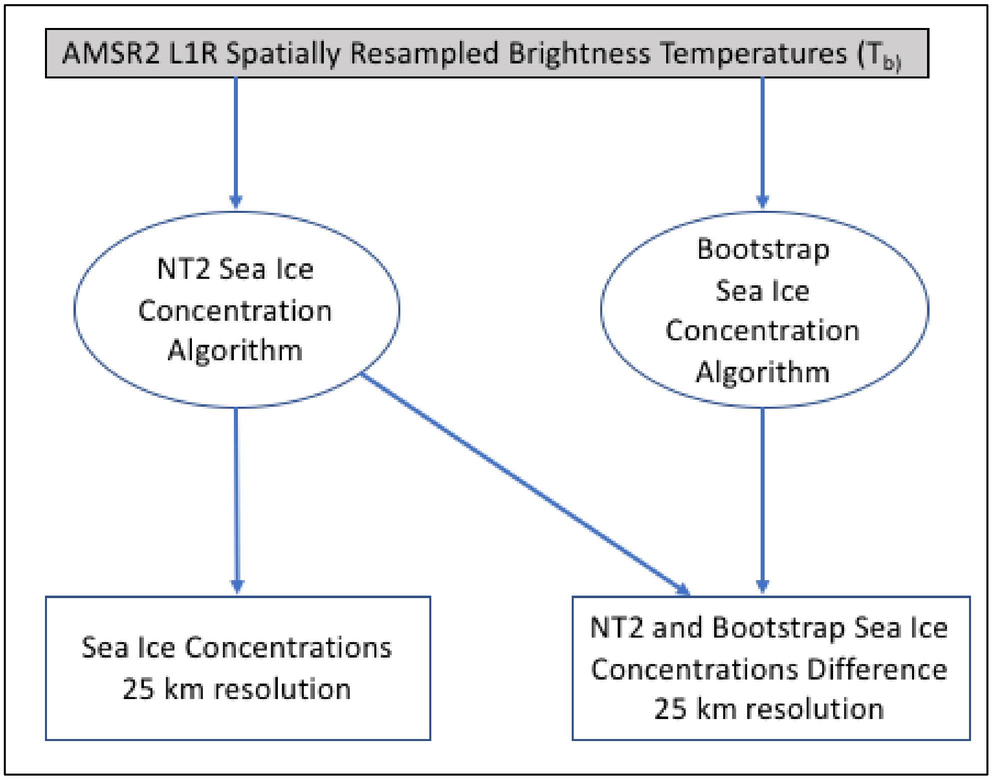

Figure 8. Source and algorithms used to create AMSR2 25 km sea ice concentration difference grids.

2.3 Quality, Errors, and Limitations

2.3.1 Assessment

Each HDF-EOS5 data file contains core metadata with Quality Assessment (QA) metadata flags that are set by the operational processing code run by the AMSR Science Investigator-led Processing System (SIPS) prior to delivery to NSIDC. A separate metadata file in XML format is also delivered to NSIDC with the HDF-EOS file. This file contains the same quality assessment (QA) metadata flags as the core metadata contained in the HDF-EOS file. Three levels of QA are applied to AMSR2 files: automatic, operational, and science. Please note that if a granule passes automatic QA and operational QA, the granule is forwarded to NSIDC for archive and distribution. If not, the issue is resolved and the granule is reprocessed. Science QA is performed automatically during nominal processing, but only reviewed closely after-the-fact in conjunction with questions that arise after processing is complete.

2.3.2 Automatic QA

Out-of-bounds L1R T_bs are screened out before T_bs are interpolated to the 25 km grid.

2.3.3 Operational QA

AMSR2 L1R data are subject to operational QA by JAXA prior to arriving at the AMSR SIPS for processing to higher-level products. Operational QA varies by product, but it typically checks for the following criteria in a given file (Conway 2002):

- File is correctly named and sized
- File contains all expected elements
- File is in the expected format
- Required EOS fields of time, latitude, and longitude are present and populated
- Structural metadata is correct and complete
- The file is not a duplicate
- The HDF-EOS version number is provided in the global attributes
- The correct number of input files were available and processed.

2.3.4 Science QA

In the SIPS environment, as part of the processing code, the science QA includes checking the maximum and minimum variable values, and percent of missing data and out-of-bounds data per variable value. At the Science Computing Facility (SCF), co-located with the SIPS, post-processing science QA involves reviewing the operational QA files and browse images, and performing the following additional QA procedures (Conway 2002):

- Historical data comparisons
- Detection of errors in geolocation
- Verification of calibration data
- Trends in calibration data
- Detection of large scatter among data points that should be consistent

Several tools have been developed to aid in the QA process of the Level 3 AMSR2 products. The Team Lead SIPS (TLSIPS) provides the browse image software. This creates a QA browse image in Portable Network Graphics (PNG) format available for visual QA. The Team Lead SCF (TLSCF) provides metadata and QA software specific to each product that provides the metadata files discussed above and a QA summary report in text format. The products of these tools are provided to NSIDC DAAC along with each data granule.

2.3.5 Accuracy and Precision

Refer to the ATBD for information about data used to check the accuracy and precision of AMSR2 observations.

2.3.6 Anomalies

Refer to the AMSR2 NRT Anomalies Page for information regarding data anomalies or gaps in coverage. Updates to this page may be forthcoming.

2.4 Instrumentation

2.4.1 Description

For detailed a description of the AMSR2 instrument, refer to the AMSR2 Channel Specification and Products page.

3 CONTACTS AND ACKNOWLEDGMENTS

Josefino Comiso and **Thorsten Markus**
Cryospheric Sciences Laboratory
NASA Goddard Space Flight Center

4 REFERENCES

Meier, W. N., Markus, T., Comisco, J., Ivanoff, I and J. Miller. 2017. Algorithm Theoretical Basis Document (ATBD): AMSR2 Sea Ice. AMSR2 Project, NASA Goddard Space Flight Center, Greenbelt, MD. (PDF)

Meier, W. N. and https://nsidc.org/sites/nsidc.org/files/technical-references/AMSR2_SeaIce_ATBD_V2.pdfA. Ivanoff. 2017. Intercalibration of AMSR2 NASA Team 2 algorithm sea ice concentrations with AMSR-E slow rotation data. *IEEE Journal Special Topics Application Earth Observation & Remote Sensing* 10(8). https://doi.org/10.1109/JSTARS.2017.2719624.

T. Maeda, Y. Taniguchi, and K. Imaoka. 2016. GCOM-W1 AMSR2 Level 1R Product: Dataset of Brightness Temperature Modified Using the Antenna Pattern Matching Technique. *IEEE Transactions on Geoscience and Remote Sensing*, 54(2), 770-782. https://doi.org/10.1109/TGRS.2015.2465170.

Markus, T. and D.J. Cavalieri. 2009. The AMSR-E NT2 sea ice concentration algorithm: its basis and implementation. *Journal of The Remote Sensing Society of Japan* 29(1), 216-225, https://doi.org/10.11440/rssj.29.216.

Comiso, J. C. 2009. Enhanced sea ice concentration and ice extent from AMSR-E Data. *Journal The Remote Sensing Society of Japan* 29(1), 199-215. https://doi.org/10.11440/rssj.29.199.

Comiso, J. C., and F. Nishio. 2008. Trends in the Sea Ice Cover Using Enhanced and Compatible AMSR-E, SSM/I, and SMMR Data. *Journal of Geophysical Research* 113, C02S07, doi:10.1029/2007JC0043257.

Conway, D. 2002. Advanced Microwave Scanning Radiometer - EOS Quality Assurance Plan. Huntsville, AL: Global Hydrology and Climate Center.

Markus, T. and Cavalieri, D. J. 2000. An Enhancement of the NASA Team Sea Ice Algorithm. *IEEE Transactions on Geoscience and Remote Sensing* 38, 1387-1398. https://doi.org/10.1109/36.843033.

Comiso, J. C., Cavalieri, D. J., and T Markus. 2003. Sea Ice Concentration, Ice Temperature, and Snow Depth using AMSR-E data. *IEEE Transactions on Geoscience and Remote Sensing* 41(2), 243-252. https://doi.org/10.1109/TGRS.2002.808317.

Comiso, J. C., Cavalieri, D. J., Parkinson, C. L., and P Gloersen. 1997. Passive microwave algorithms for sea ice concentration - A comparison of two techniques. *Remote Sensing of Environment* 60(3), 357-384. https://doi.org/10.1016/S0034-4257(96)00220-9.

Comiso, J. C. 1986. Characteristics of Winter Sea Ice from Satellite Multispectral Microwave Observations. *Journal of Geophysical Research* 91(C1), 975-994.

Cavalieri et al. 1995. Reduction of Weather Effects in the Calculation of Sea Ice Concentration with the DMSP SSM/I. *Journal of Glaciology* 41(139), 455-464. https://doi.org/10.3189/S002214300003479.

Kummerow, C. 1993. On the accuracy of the Eddington approximation for radiative transfer in the microwave frequencies. *Journal Geophysical Research* 98(D2), 2757-2765. https://doi.org/10.1029/92JD02472.

Eppler, et al. 1992. Passive Microwave Signatures of Sea Ice in Microwave Remote Sensing of Ice. *Geophysical Monograph*, 68: 47-71. https://doi.org/10.1029/GM068p0047.

Gloersen P. and D.J. Cavalieri. 1986. Reduction of Weather Effects in the Calculation of Sea Ice Concentration from Microwave Radiances. *Journal of Geophysical Research* 91(C3), 3913-3919. https://doi.org/10.1029/JC091iC03p03913.

Matzler, C., Ramseier, R.O., and E. Svendsen. 1984. Polarization effects in sea ice signatures. *IEEE Journal. Oceanic Eng* 9, 333-338.

Fraser et al. 1975. Interaction Mechanisms Within the Atmosphere Including the Manual of Remote Sensing. *American Society of Photogrammetry* 181-233. Falls Church, VA.

G. E. Backus, J. F. Gilbert. 1967. Numerical Applications of a Formalism for Geophysical Inverse Problems. *Geophysical Journal International* 13(1-3), 247–276. https://doi.org/10.1111/j.1365-246X.1967.tb02159.x.

5 DOCUMENT INFORMATION

5.1 Publication Date

09 July 2018

5.2 Date Last Updated

15 March 2021